

# Cuff-less Estimation of Blood Pressure from Vibrational Cardiography using a Convolutional Neural Network

James Skoric<sup>1</sup>, Yannick D’Mello<sup>1</sup>, Nathan Clairmonte<sup>1</sup>, Angus McLean<sup>1</sup>, Siddiqui Hakim<sup>1</sup>, Ezz Aboulezz<sup>1</sup>, Michel Lortie<sup>2</sup>, David V. Plant<sup>1</sup>

<sup>1</sup>McGill University, Montreal, Canada

<sup>2</sup>MDA Corporation, Ottawa, Canada

## Abstract

*Wearable monitoring is important for the diagnosis, prevention, and treatment of cardiovascular diseases and overall cardiac health. A key indicator, Blood pressure (BP), currently relies on cuff-based devices for measurement that are cumbersome for ambulatory monitoring scenarios. Vibrational cardiography (VCG) is an unobtrusive, non-invasive tool which records cardiac vibrations on the surface of the chest. This work proposes using VCG in a novel method to estimate BP from a single point of contact. VCG was recorded by an inertial measurement unit on the xiphoid process of 62 subjects. A convolutional neural network was trained on the VCG waveforms to estimate systolic and diastolic BP. This resulted in an  $r$ -squared correlation coefficient of 0.86 and 0.89 and a mean-absolute-error of 3.4 mmHg and 2.2 mmHg for systolic and diastolic BP, respectively. Therefore, this work shows the applicability of using exclusively VCG for BP estimation. It affirms the value of VCG as an all-purpose health monitor, while also improving on the current techniques for continuous BP monitoring. This indicates the potential of VCG in many forms of wearable monitoring including remote healthcare, fitness, and wellness monitoring.*

## 1. Introduction

Blood pressure (BP) an important vital sign for monitoring cardiac health. It is used as a predictor for cardiovascular disease and overall mortality [1]. This makes it a valuable metric in many forms of healthcare from the intensive care unit, annual checkups, and even at-home monitoring [2]. Despite its necessity, current BP monitoring methods require a cumbersome cuff-based device which is obstructive to daily life and only offers discrete, discontinuous measurements. Therefore, to facilitate wearable and remote monitoring, there has been a push towards cuff-less monitoring. Several of these recent advances include inflatable wrist devices, weighing

scales, and other wearables [3].

One wearable monitoring technique is vibrational cardiography (VCG) which records cardiac vibrations on the surface of the chest from an inertial measurement unit (IMU). The method records both linear acceleration, known as seismocardiography (SCG) and rotational velocity, known as gyrocardiography (GCG). VCG contains many applications in cardiac monitoring with its ability to measure heart rate [4], cardiac time intervals [5], and respiratory information [6]. Recent studies have applied VCG to derive information on stroke volume [7], arrhythmias [8], and even predicting heart failure [9].

A high correlation between the fiducial points of VCG and the timing of the opening and closing of valves indicates that valve movement could be considered one of the origins of the vibrational signal. This motion of the valves is controlled by the pressure differentials between the ventricle and the aorta during the cardiac cycle. Therefore, as VCG is generated by cardiac valve motion and the hydraulic valve motion is caused by central hemodynamics, there is an indirect relationship between VCG and blood pressure. The difficulty in deriving this relationship lies in the fact that VCG is highly variable due to the imperfect nature of the structural, electrical, and fluidic systems of the body.

Due to advances in computational methods, machine learning (ML) excels at deriving statistical relationships within complex systems. Other studies have estimated BP from wearable cardiography techniques using ML [10]. Thanks to its small form factor and centralized location, VCG is a more attractive solution. Therefore, we have used an ML model to estimate BP using VCG. This paper shows the development of a convolutional neural network, and its proficiency as a tool in systolic and diastolic blood pressure estimation.

## 2. Methods

### 2.1 Data Acquisition

The data was recorded using a custom-assembled

system consisting of commercial, off the shelf parts. The system was composed of a single IMU (MPU9250, Invensense) which contained an integrated accelerometer and gyroscope. The IMU was polled via I2C protocol by a Raspberry Pi zero. The sampling rate was approximately 600 Hz. The accelerometer and gyroscope were set to a range of  $\pm 2$  g and  $\pm 250$  deg, respectively. Data was saved to a text file on the Raspberry Pi and was then sent wirelessly to a laptop computer for post-processing. A Biopac MP160 was used as a reference device containing the electrocardiography (ECG) and non-invasive blood pressure (NIBP) modules, which was sent to a second laptop. An externally wired clock signal was sent from the Biopac to the Raspberry Pi to synchronize the two devices.

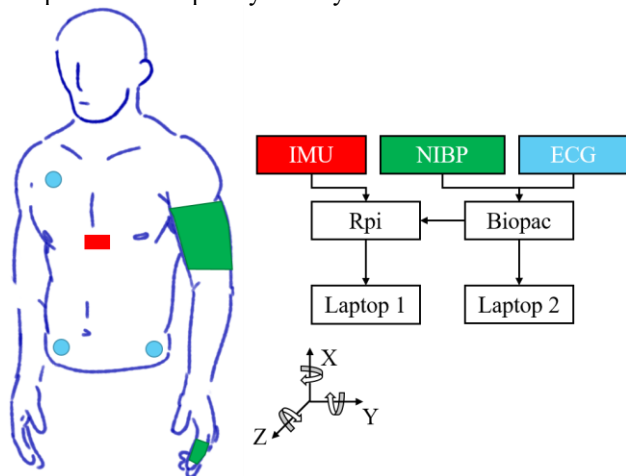


Figure 1. System schematic showing the IMU (red), ECG (blue), and NIBP (green) sensor locations on the body with corresponding connections to the Raspberry Pi (Rpi) and Biopac systems.

The experiment was conducted on 62 subjects. All data was collected at McGill University and was approved by the McGill Research Ethics Board. The study consisted of 35 male and 27 female subjects with (average  $\pm$  standard deviation) age:  $24.6 \pm 4.5$  years, height:  $172 \pm 10.4$  cm, and weight:  $70.2 \pm 16.3$  kgs. All subjects were healthy and had no known prior cardiovascular, respiratory, or hemodynamic conditions. Subjects were recorded in the supine position. The IMU was secured to the xiphoid process with a piece of double-sided tape with the X, Y, and Z axes oriented in the longitudinal, horizontal, and dorsoventral axes of the body, respectively. The gyroscope was left-hand oriented around each respective axis. Three ECG electrodes were placed across the torso with the positive electrode near the right arm, negative near the left leg and ground near the right leg. The NIBP device was secured to the left wrist using the finger cuffs on the index and middle fingers. For calibration, an inflatable arm cuff was placed on the left bicep.

First, the NIBP device was calibrated to the arm. Subjects were asked to stay motionless and breathe

normally. Then the subjects lay still for a 3-minute recording. The trial then consisted of several tests that were not used in this study. Afterwards they completed another 2-minute baseline recording, totalling 5-minutes of data per subject.

## 2.2 Preprocessing

The NIBP signal was filtered by a 10 Hz low pass filter built into the Biopac device. The Biopac AcqKnowledge software was used to annotate the R-peaks from the ECG waveform. Artifact samples due to sensor noise were removed and filled by interpolation. It was then filtered by a 5<sup>th</sup> order Butterworth filter with a 90 Hz cut-off. The VCG signals were resampled to 200 Hz. An example of the VCG signal, from a single subject, can be seen in Figure 2. The signals were segmented into cardiac cycles, starting at 0.1 seconds before the ECG R-peak. The corresponding maximum in the NIBP signal during each cardiac beat was defined as the systolic blood pressure (SBP) and likewise the minimum was the diastolic blood pressure (DBP).

To prepare the sample for the ML model, each heartbeat was post mean-padded to a length of 500 points, corresponding to a maximum beat-to-beat duration 2.5 seconds, which was longer than that observed for all subjects. All six axes were inputted to the model, resulting in a 500-by-6 vector for each training instance. The output for each instance was a single scalar value, corresponding to either SBP or DBP. A separate model was trained for each BP metric. Heartbeats containing major artifacts in BP or VCG, generally corresponding to motion or poor signal quality, were discarded from the study.

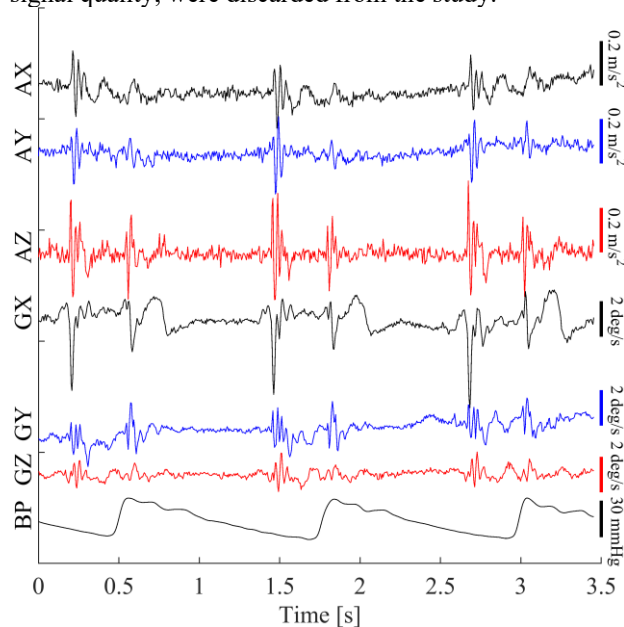


Figure 2. An example of VCG showing the acceleration in the X, Y, and Z axes (AX, AY, AZ), gyration in the X, Y, and Z axes (GX, GY, GZ), and corresponding finger BP.

### 2.3 Model

A one-dimensional convolutional neural network (CNN) model was built with a similar structure to the VGG16 model [11]. The structure was simplified to improve generalizability. The layout is shown in Figure 3. The model was sequential and consisted of three convolution blocks. Each block had two or three six-channel convolutional layers followed by a max pooling layer with a pooling size of 2. All one-dimensional convolutional layers had a kernel size of 3, same padding to retain output shape, and ReLU activation. The number of filters per convolution layer increased in each convolution block. Finally, there was a flatten layer and two fully connected dense layers for output. The model was built and trained using the Keras framework in python. It was trained to minimize the mean-squared-error loss function using an Adam optimizer with a batch size of 128 and 100 epochs.

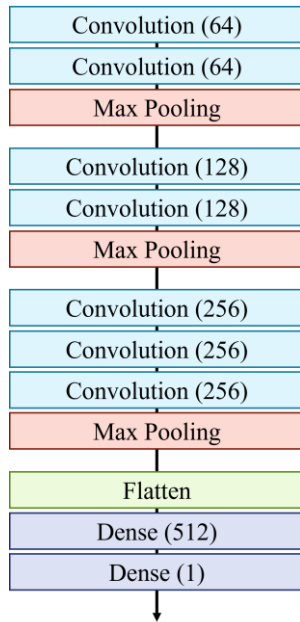


Figure 3. Structure of the proposed CNN. Model layers are shown with the corresponding number of filters for each convolutional layer and the number of nodes for each dense layer.

### 2.4 Validation

The proposed model was trained using 80% of the data and tested with 20%. All of the data was shuffled and subsequently split randomly. Pearson’s squared correlation coefficient ( $r^2$ ) was used to validate linearity between estimated and actual blood pressure.

### 3. Results

The analysis was performed on 62 subjects with 18,330 heartbeats corresponding to 17,224 seconds of data. The average SBP observed was  $115.5 \pm 12.9$  mmHg. The average DBP observed was  $66.7 \pm 9.2$  mmHg. The evaluated CNN model produced an  $r^2$  of 0.86 ( $p < 0.001$ ) for SBP and 0.89 ( $p < 0.001$ ) for DBP. The corresponding mean-absolute-error (MAE) was 3.4 mmHg and 2.2 mmHg for SBP and DBP, respectively. Figure 4 shows a Bland-Altman plot for estimated SBP and DBP, with respective 95% limits of agreement of -9.21 to 9.88 mmHg and -6.51 to 5.41 mmHg.

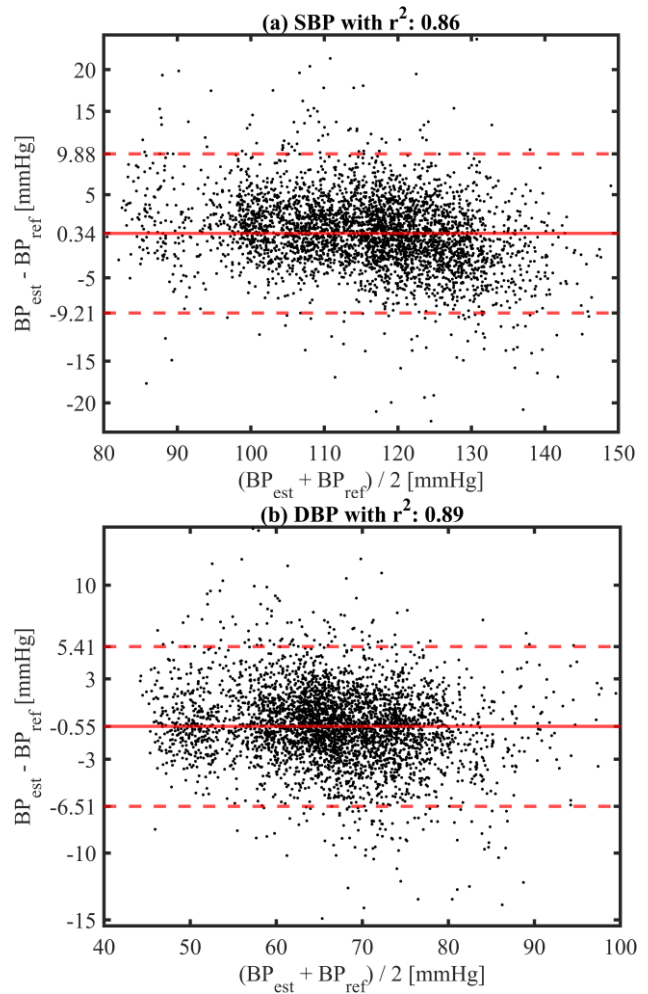


Figure 4. Bland Altman plots of estimated blood pressure ( $BP_{est}$ ) and reference blood pressure ( $BP_{ref}$ ) with mean (solid red) and 95% limits of agreement (dashed red) for (a) SBP and (b) DBP.

## 4. Discussion and Conclusion

The model was able to estimate both SBP and DBP with a high correlation to the reference finger cuff, shows a relationship between the VCG signal and BP. Current standards by the Association for the Advancement of Medical Instrumentation (AAMI) describe a performance of less than 5 mmHg mean error and less than 8 mmHg standard deviation [12]. The proposed model performed within these guidelines with 0.34 and  $-0.55$  mmHg mean error, and 4.8 and 3.0 mmHg standard deviation for SBP and DBP, respectively. The achieved low error and high correlation confirm the ability of using VCG as a robust vital signs monitor, capable of measuring heart rate, respiration, and now BP from a single point of contact on the body. This integration of multiple monitoring metrics gives VCG an edge over traditional techniques due to the improved ease of use.

While the results are statistically verified, this study has a few limitations. First, the study incorporated random shuffling of the heartbeats, meaning that causality is not preserved, indicating that the model could be using future instances to predict prior BP. In comparison to other works, this is a common occurrence in the field of study and therefore the performance of the model should be evaluated using only prior information to simulate a real-world environment. Second, the model was optimized to the subjects within the study. The performance on an unseen subject was not investigated. This would certainly reduce the prediction accuracy given that VCG morphology has a large inter-subject variability. Further work should be explored to provide generalized results on a less overfit model. Finally, the study did not examine long-term measurements and only included healthy subjects in an ideal environment without outside sources of noise. Given the goal of implementing this system in wearable scenarios, future studies should include more challenging situations, such as movement, exercise, and daily activities, to test the practical utility of the approach.

This work has opened the door to using VCG for hemodynamic monitoring. It has provided a basis for estimating BP that can be extended to models and situations. The analytical causation behind the VCG-BP relationship can be examined further to form more verifiable estimations for use in health, wellness, and fitness monitoring.

## Acknowledgments

This work was supported in part by the National Sciences and Engineering Research Council (NSERC) of Canada, MDA Corporation, and McGill University

## References

[1] W. B. Kannel, "Blood pressure as a cardiovascular risk

- factor: prevention and treatment," *Jama*, vol. 275, no. 20, pp. 1571-1576, 1996.
- [2] T. G. Pickering, N. H. Miller, G. Ogedegbe, L. R. Krakoff, N. T. Artinian, and D. Goff, "Call to action on use and reimbursement for home blood pressure monitoring: executive summary: a joint scientific statement from the American Heart Association, American Society Of Hypertension, and Preventive Cardiovascular Nurses Association," *Hypertension*, vol. 52, no. 1, pp. 1-9, 2008.
- [3] J. Solà and R. Delgado-Gonzalo, "The Handbook of Cuffless Blood Pressure Monitoring," *Springer*, vol. 1007, pp. 978-3, 2019.
- [4] Y. D'Mello *et al.*, "Real-Time Cardiac Beat Detection and Heart Rate Monitoring from Combined Seismocardiography and Gyrocardiography," *Sensors*, vol. 19, no. 16, p. 3472, 2019.
- [5] D. M. Quarrie and P. Neary, "Comparison of seismocardiography to echocardiography for measuring cardiac cycle events," 2011.
- [6] J. Skoric *et al.*, "Relationship of the Respiration Waveform to a Chest Worn Inertial Sensor," in *2020 42nd Annual International Conference of the IEEE Engineering in Medicine & Biology Society (EMBC)*, 2020, pp. 2732-2735: IEEE.
- [7] B. Semiz *et al.*, "Non-Invasive Wearable Patch Utilizing Seismocardiography for Peri-Operative Use in Surgical Patients," *IEEE Journal of Biomedical and Health Informatics*, vol. 25, no. 5, pp. 1572-1582, 2020.
- [8] O. Lahdenoja *et al.*, "Atrial fibrillation detection via accelerometer and gyroscope of a smartphone," *IEEE Journal of Biomedical and Health Informatics*, vol. 22, no. 1, pp. 108-118, 2017.
- [9] O. T. Inan *et al.*, "Novel wearable seismocardiography and machine learning algorithms can assess clinical status of heart failure patients," *Circulation: Heart Failure*, vol. 11, no. 1, p. e004313, 2018.
- [10] C. El-Hajj and P. A. Kyriacou, "A review of machine learning techniques in photoplethysmography for the non-invasive cuff-less measurement of blood pressure," *Biomedical Signal Processing and Control*, vol. 58, p. 101870, 2020.
- [11] K. Simonyan and A. Zisserman, "Very deep convolutional networks for large-scale image recognition," *arXiv preprint arXiv:1409.1556*, 2014.
- [12] *American national standard: electronic or automated sphygmomanometers, ANSI/AAMI SP10-2002*, 2003.

Address for correspondence:

James Skoric  
Room 848, McConnell Engineering Building,  
3480 University Street, McGill University  
Montreal, QC H3A 2A7 Canada  
james.skoric@mail.mcgill.ca